New Mexico Geological Society

Downloaded from: https://nmgs.nmt.edu/publications/guidebooks/37



Tin deposits in the Black Range district

Charles H. Maxwell, Eugene E. Foord, Mariel R. Oakman, and D. B. Harvey
1986, pp. 273-281. https://doi.org/10.56577/FFC-37.273

in:

Truth or Consequences Region, Clemons, R. E.; King, W. E.; Mack, G. H.; Zidek, J.; [eds.], New Mexico Geological Society 37th Annual Fall Field Conference Guidebook, 317 p. https://doi.org/10.56577/FFC-37

This is one of many related papers that were included in the 1986 NMGS Fall Field Conference Guidebook.

Annual NMGS Fall Field Conference Guidebooks

Every fall since 1950, the New Mexico Geological Society (NMGS) has held an annual Fall Field Conference that explores some region of New Mexico (or surrounding states). Always well attended, these conferences provide a guidebook to participants. Besides detailed road logs, the guidebooks contain many well written, edited, and peer-reviewed geoscience papers. These books have set the national standard for geologic guidebooks and are an essential geologic reference for anyone working in or around New Mexico.

Free Downloads

NMGS has decided to make peer-reviewed papers from our Fall Field Conference guidebooks available for free download. This is in keeping with our mission of promoting interest, research, and cooperation regarding geology in New Mexico. However, guidebook sales represent a significant proportion of our operating budget. Therefore, only *research papers* are available for download. *Road logs*, *mini-papers*, and other selected content are available only in print for recent guidebooks.

Copyright Information

Publications of the New Mexico Geological Society, printed and electronic, are protected by the copyright laws of the United States. No material from the NMGS website, or printed and electronic publications, may be reprinted or redistributed without NMGS permission. Contact us for permission to reprint portions of any of our publications.

One printed copy of any materials from the NMGS website or our print and electronic publications may be made for individual use without our permission. Teachers and students may make unlimited copies for educational use. Any other use of these materials requires explicit permission.

This page is intentionally left blank to maintain order of facing pages.

TIN DEPOSITS IN THE BLACK RANGE TIN DISTRICT

C.H. MAXWELL[1], E.E. FOORD[1], M.R. OAKMAN[2], and D.B. HARVEY[3]
[1]U.S. Geological Survey, Box 25046, M.S. 905, Federal Center, Denver, CO 80225; [2]Department of Oceanography, University of Rhode Island, Narragansett, RI 02882; [3]5212 Highland Avenue, Yorba Linda, CA 92686

Abstract—The Black Range tin district is in the eastern part of the Datil–Mogollon volcanic field, in Catron and Sierra Counties, southwestern New Mexico. Host for the tin deposits is the Oligocene Taylor Creek Rhyolite and associated pyroclastic rocks. The high-silica, I-type rhyolite is peraluminous, moderately evolved, contains about 1% normative corundum, and normative albite plus anorthite about equal to orthoclase. The rhyolite is porphyritic, with sanidine and quartz phenocrysts. Tin was deposited in a near-surface volcanic environment characterized by extreme temperature and pressure gradients. Conditions of tin deposition were variable from locality to locality, ranging from high-temperature, vapor-dominated systems to low-temperature and pressure, fluid-dominated systems. Cassiterite occurs in lithophysae and miarolitic cavities, in gash veins and veinlets, in veins and stockworks of reticulate veinlets, and disseminated in altered rock. The most abundant form of cassiterite is wood-tin. Nearly as abundant is dark-red cassiterite, pseudomorphic after hematite, and in bladed aggregates intergrown with hematite. Less common are euhedral crystals or aggregates of crystals. The cassiterite varies from essentially pure SnO_2 to material with as much as 10 wt% of Fe, Sb, As, Zn, In, Si, and other elements. Commonly associated minerals include hematite, pseudobrookite, bixbyite, topaz, sanidine, clinopyroxene, durangite, beudandite, hidalgoite, jarosite, alunite, heulandite, cristobalite, tridymite, quartz, chalcedony, opal, fluorite, cryptomelane, smectite, todorokite, and varlamoffite. Very sparse amounts of several new antimonates, arsenates, and fluoroarsenates occur at at least one locality. Almost all of the tin produced in the district was wood-tin nuggets from placer or colluvial deposits. A small proportion of the tin apparently was derived from flow domes, but the majority most likely came from conduit and underlying intrusives. Deuteric fluids from these intrusives may have interacted to varying extent with meteoric ground water. Some of the wood-tin is of supergene origin.

INTRODUCTION

The Black Range tin district has been the subject of numerous studies for more than 60 years. Placer tin was discovered in Squaw Creek in 1909 (Fries 1940) and along Taylor Creek in 1918 (Hill 1921). Several vein deposits were located in 1919 in Taylor Creek and Squaw Creek, and in 1920 at Hardcastle Creek and the Kemp Mesa–Beaver Creek area. Prospecting and claim development have continued sporadically to the present. Detailed geologic studies of the Taylor Creek and Squaw Creek deposits were made by Fries (1940) and Fries & Butler (1943), and concurrent resource studies were reported by Volin et al. (1947). Lufkin (1972, 1976, 1977) conducted detailed studies of the tin mineralization in the area; his study was followed by several general geologic studies of the area (Correa 1980, 1981, Eggleston in preparation, Goerold 1981, Harvey 1985, Lawrence 1985). This paper is a summary of the results obtained to date from ongoing studies of tin deposits in the Black Range.

The tin-bearing area was named the Taylor Creek district by Hill (1921). The use of the name was continued by Harley (1934: 67) and File & Northrop (1966). Fries (1940) tacitly restricted that name to those deposits near Taylor Creek and used the name Black Range tin district on the map of the region (Fries & Butler 1943). The southern part of the Black Range tin district is included in the northern part of the Aldo Leopold Wilderness (formerly Black Range Primitive Area), and a potential northwest extension of the district is in the Continental Divide Wilderness Study Area. Most of the district is National Forest land west of the continental divide, straddling NM-59.

The district (Fig. 1) is approximately 50 km × 10–25 km, at an average elevation of 2,378 m, in Sierra and Catron Counties. Total production from the district is not known, but several shipments of tin concentrates have been recorded: 1,863 lbs in 1937–40 (Fries 1940), an estimated 21,900 lbs between 1940 and 1943 (Volin et al. 1947), 40,000 lbs in 1965–69 (Harvey 1985), and unverified reports of about 74,000 lbs in the late 1960's and early 1970's. The concentrates contain 45–50% metallic tin and may contain several percent in aggregate of lead, zinc, antimony, and arsenic.

Lode deposits were discovered early in the history of the district, but of the tin produced almost all has been from placer and colluvial accumulations. Economic placers have been restricted in size because the relatively primitive methods of gravity separation used in the area

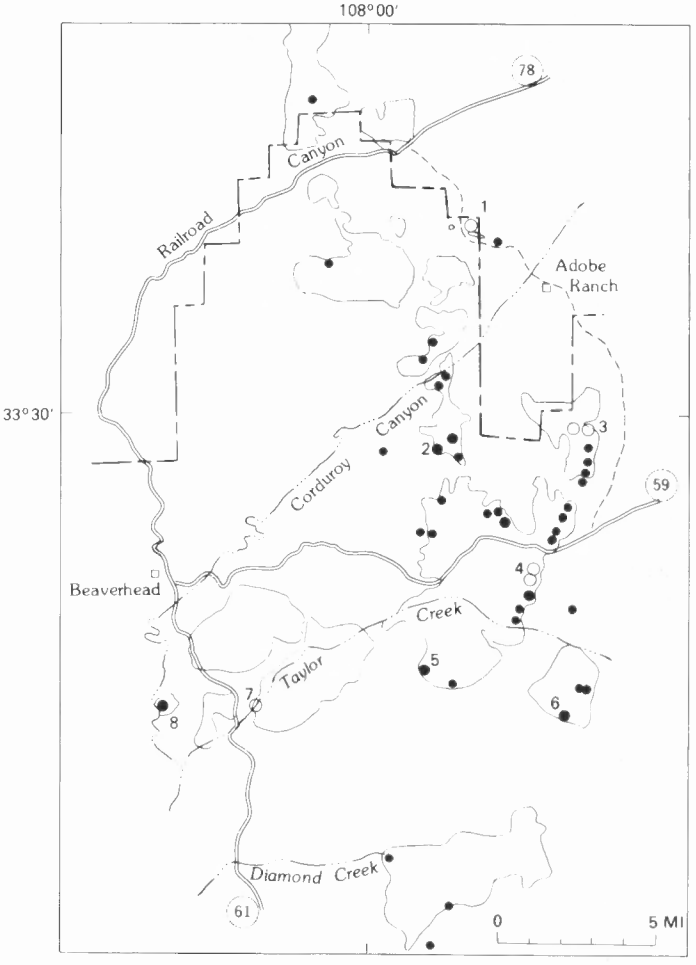


FIGURE 1—Sketch map of Black Range tin district. Patterned areas show approximate distribution of Taylor Creek Rhyolite. Small dots represent minor occurrences of tin, larger dots those of small deposits, and open circles those of major deposits. Numbers refer to localities discussed in text. Arrows indicate locations of field-trip stops.

were inefficient on particles smaller than 2–3 mm in diameter. The energy of most streams in the region, even with flash floods, is too low to carry very far the particles of cassiterite and wood-tin larger than approximately 1 cm. Thus, most of the rich placers are colluvial and directly overlie the veins that produced the tin, or are only a few tens of meters downstream. The smallest cassiterite crystals might be carried many kilometers downstream, but do not seem to concentrate into workable placers in spite of a specific gravity near 7. Test results show that the small cassiterite crystals, especially the wood-tin and acicular varieties, are not very resistant to abrasion and are quickly ground into slime in the larger streams, then diluted and widely dispersed.

Most of the economic placer deposits are now largely worked out, and such deposits are not shown on the maps. Most of the following discussion is of the lode deposits.

The Black Range tin district is in the eastern part of the mid-Tertiary Mogollon–Datil volcanic field, which is composed of many different intermediate to felsic volcanic-rock units and volcaniclastic rocks of both local and regional extent. They have been mapped, named, and described in numerous publications (Elston 1968, Eggleston & Norman 1983, Lawrence & Richter 1985, Ratté et al. 1984). Most of the tin mineralization is in the Taylor Creek Rhyolite, although some of the occurrences of tin are in older and younger rocks.

TAYLOR CREEK RHYOLITE

The Taylor Creek Rhyolite occurs as a series of isolated or overlapping flow domes ranging in diameter from about 400 m to 5 km, and as associated pyroclastic rocks. The domes have irregularly fan-shaped flow layering near their centers, which grades to flat and variably contorted layering around the edges. Basal and interspersed flow breccias and local overlying carapace breccias, froth flows (Smith 1960: 208), and pyroclastic rocks are common. Most of the domes have an early-stage shield of pyroclastic rocks which may be thin and smaller than the dome itself, or may cover an area many times the area of the associated dome, such as the tuff of Garcia Camp underlying the Indian Peaks dome (Lawrence & Richter 1985). The pyroclastic shield is commonly distorted by the bulldozing action of the encroaching flows, and locally may be picked up and incorporated into the dome structure. These incorporated pyroclastic xenoliths are as large as 30 m in diameter. Froth flows are locally common and are composed of glass, pumice, and shards with flat and contorted flow lines wrapped around sanidine and quartz phenocrysts; they range from essentially unwelded to intensely welded and resemble ash-flow tuff. The rhyolite and pyroclastic rocks are generally porphyritic, but have a wide variation in size and quantity of phenocrysts. The phenocrysts are sanidine (Or_{50-55}) and quartz, and the groundmass of the flows is very fine-grained granophyric to glassy, variably devitrified, commonly cryptocrystalline, in spherulitic or banded forms with vague sweeping aggregate polarization, or microcrystalline with poorly defined polarization. Many of the flow units, especially in the upper and outer levels of the domes, have abundant, concentrically layered lithophysae or irregular, angular miarolitic cavities, or both, and these units generally exhibit vapor-phase crystallization. The rhyolite in many areas has been recrystallized by vapor-phase processes and is characterized by the presence of euhedral crystals of sanidine, quartz, tridymite, pseudobrookite, bixbyite, and topaz in the cavities (Fries et al. 1942, Lufkin 1976). Red beryl also occurs at one locality (Stop 5 of First Day) (Kimbler & Haynes 1980).

Zones of intense vapor-phase alteration are locally common but sporadic in occurrence, and are generally found toward the interior of the domes. They are relatively small in size, a few meters to 100 m in diameter. One characteristic area is just southwest and down the hill from Stop 5 of First Day. The rock in the altered zones is stark white, soft, and powdery; sanidine phenocrysts are unchanged or have minor overgrowths of the same mineral, and the quartz is corroded and embayed. Centers of altered zones are composed of a very fine-grained to clay-sized aggregate of sanidine with intergrown sanidine and cristobalite toward the edges. Accessory mineral content is variable and consists of scattered tiny, red, translucent, hematite crystals or sparse to abundant specularite, and locally abundant pseudobrookite and bixbyite.

Comparison of major-oxide and minor- and trace-element analyses of the vapor-phase-altered rocks and nearby equivalent vitrophyres with only slight devitrification reveals little change in composition (Tab. 1). SiO_2 contents are 1–2% less and loss-on-ignition (LOI) is doubled in the vapor-phase-altered rocks. Other oxides are relatively unchanged as compared to the vitrophyres. Vapor-phase-altered rocks have local overprints of argillic alteration and many changes in composition are evident. In these hydrothermally altered rocks, the SiO_2 and Al_2O_3 are each 4–5% less, Na_2O and K_2O are each 3–4% less, CaO is several percent more, LOI increases by a factor of five or more, and some trace elements (F, As, Ba, La, Pb, Sn, Sr, Y, Ce, and Li) increase by factors of three to ten. Most of the argillically altered rocks are associated with tin mineralization; one notable exception is the Continental Divide clay pit (Optional Stop 2 of First Day).

Ten of the samples used in this report were collected by Bruce Reed (USGS, Alaska); additional 16 samples were collected by the authors. Localities are shown in Fig. 2; numbers refer to eight samples of porphyritic rhyolite with minimum alteration and devitrification which were selected for K–Ar dating (Tab. 2). Fig. 3 is a Harker diagram of analyses from Tab. 1. One sample from the Willow Creek deposit, Monticello tin area, is included for comparison. Note that the range of SiO_2 for unaltered rocks is less than 2%. The range for rocks showing vapor-phase crystallization and/or minor alteration is less than 3%. The other oxides show only minor variation.

The Taylor Creek Rhyolite is an I-type, high-silica, peraluminous (Fig. 4), moderately evolved rhyolite containing normative corundum (about 1%), and has equal contents of normative albite plus anorthite and orthoclase (Fig. 5). The high SiO_2 content and the trace- and minor-element geochemistry, such as very low Ba, Sr, and Ca content and relatively high Rb, Nb, Th, and U content, are indicative of the degree of evolution of the rhyolite. Calculated values for both fresh and altered rock cluster to the Or-rich side of the 0.5 kb ternary minimum melting compositions on an Q–Ab–Or plot. AFM, ACF, and A′KF diagrams for all of the rock samples are shown in Fig. 6. Mole values on all three plots cluster about points removed from those of average granite and tin granite. This rhyolite is similar to the topaz rhyolites described by Burt et al. (1982) and Christiansen et al. (1983), but contains less fluorine (0.04% versus 0.3%), alumina, soda, and lime, and slightly more silica and iron (Fig. 3). The average contents of both Cl and CO_2 are less than 0.01%. The Taylor Creek Rhyolite is significantly enriched in As, Sb, Rb, REE, and U and depleted in Ca, Sr, Ba, Eu, and P relative to average granite (Krauskopf 1979) (Fig. 7). Co, Ni, and Sn are neither enriched nor depleted. Rare-earth patterns are similar to those of topaz rhyolites (Christiansen et al. 1983) with a relatively flat slope (Ce/Lu = 2–3) and deep negative Eu anomaly (Fig. 8). Granitic rocks associated with tin deposits are characterized by substantial geochemical differences from the Taylor Creek Rhyolite (Tab. 3). Many major-oxide analyses of the Taylor Creek Rhyolite are available in the literature (e.g. Correa 1980, 1981, Goerold 1981, Lawrence 1985, Lufkin 1972, Richter & Lawrence 1986, Woodard 1977). Most of them differ little from the analyses obtained in the current study.

TIN DEPOSITS

The major host for the tin deposits and occurrences is the Taylor Creek Rhyolite, but one of the larger deposits (Juniper, no. 1, Fig. 1) is in the underlying tuff of Garcia Camp (Lawrence & Richter 1985) and associated tuffaceous sandstone. Several minor tin occurrences are in the tuff of Stiver Canyon (Woodard 1977), which is much older and unrelated to the Taylor Creek Rhyolite. Tin is also found in the volcanic and fluviatile conglomerate and sandstone that overlie the rhyolite. About 80% of the known resources of lode tin in the district occur in a narrow, 0.4–0.8 km wide, north–northeast-trending belt along the east side (Fig. 1, nos. 3, 4). Numerous small faults occur along and parallel to the east side of the belt (Fries & Butler 1943) and may represent reactivation along a pre-mineralization, or pre-Taylor Creek, fault now covered by rhyolite and pyroclastics.

Most of the tin deposits were formed in a near-surface volcanic environment characterized by extreme temperature and pressure gradients. The deposits are variable from locality to locality, from high-

TABLE 1—Major-oxide and trace-element analyses of Taylor Creek Rhyolite. Sample numbers 1–8 are the same as those in Tab. 2 and Fig. 2. Numbers 1A–5A are from the same units at different localities. Other sample localities are shown by symbols in Fig. 2. Major oxides determined by x-ray spectroscopy, fluorine by specific ion electrode, trace elements by various methods, including six-step semiquantitative spectrographic analysis, optical spectroscopy, and neutron activation. Analysts: A.J. Bartel, K. Stewart, J.E. Taggart, J. Seeley, D.B. Hatfield, C. Stone, E. Brandt, H. Neiman, and N.M. Conklin.

	1	1A	2	2A	3	3A	4	4A	5	5A	6	7	8
SiO_2 %	77.0	77.1	77.1	76.8	77.2	76.7	76.5	76.7	76.1	76.5	76.4	75.8	76.9
Al_2O_3%	12.0	11.9	11.7	11.9	11.6	11.7	12.2	12.1	12.2	12.1	12.1	11.7	12.0
Fe_2O_3%	1.37	1.15	1.44	1.30	1.36	1.17	1.30	1.09	1.24	1.13	1.33	2.38	1.22
Fe_2O_3%	1.15	1.08	1.13	1.13	1.22	---	0.97	0.93	1.10	1.06	1.06	1.82	1.10
FeO %	0.20	0.06	0.28	0.15	0.13	---	0.30	0.14	0.13	0.06	0.24	0.50	0.11
MgO %	0.11	<0.10	<0.10	0.16	0.13	0.18	<0.10	0.10	0.13	0.11	<0.10	<0.10	0.10
CaO %	0.23	0.31	0.18	0.21	0.22	0.21	0.17	0.15	0.21	0.14	0.30	0.09	0.18
Na_2O %	3.39	3.35	3.04	3.12	3.07	3.39	3.42	3.27	3.40	3.20	3.50	3.50	3.43
K_2O %	4.92	4.92	4.91	5.07	4.96	4.86	4.84	4.86	4.81	4.99	4.89	5.01	4.86
TiO_2 %	0.10	0.08	0.14	0.16	0.15	0.14	0.10	0.08	0.11	0.10	0.10	0.16	0.11
P_2O_5 %	<0.05	<0.05	<0.05	<0.05	<0.05	<0.05	<0.05	<0.05	<0.05	<0.05	<0.05	<0.05	<0.05
MnO %	0.06	0.03	0.03	0.04	0.04	0.03	0.02	0.02	<0.02	0.04	0.04	0.06	0.06
LOI %	0.50	0.32	0.56	0.41	0.52	0.48	0.63	0.39	0.84	0.46	0.34	0.40	0.51
F %	0.04	0.11	0.04	0.07	0.06	0.05	0.06	0.06	0.03	0.04	0.15	0.02	0.04
total%	99.47	99.26	99.10	99.22	99.30	98.91	99.21	98.80	99.06	98.80	99.12	99.06	99.40
O F %	0.02	0.05	0.02	0.03	0.03	0.02	0.03	0.03	0.01	0.02	0.06	0.01	0.02
Total%	99.45	99.21	99.08	99.19	99.27	98.89	99.18	98.77	99.05	98.78	99.06	99.05	99.38
Sn ppm	3	<4	4	<4	1	4	5	4	4	<4	3	5	1

	9	10	11	12	13	14	15	16	17	18	19	20	21
SiO_2 %	76.3	76.0	75.8	75.7	74.2	77.6	76.9	76.5	76.1	74.7	75.8	75.3	74.3
Al_2O_3%	12.1	12.0	12.3	11.8	12.6	11.7	11.7	11.8	11.7	12.3	11.5	12.2	12.3
Fe_2O_3%	1.13	1.13	1.14	1.11	1.36	1.12	1.08	1.04	1.11	1.24	1.45	1.21	1.19
Fe_2O_3%	1.11	---	---	---	---	---	1.06	1.02	1.09	1.20	1.43	---	---
FeO %	0.02	---	---	---	---	---	0.02	0.02	0.02	0.04	0.02	---	---
MgO %	0.15	0.12	0.23	0.10	0.22	0.14	0.14	0.19	0.36	0.17	0.16	0.20	0.52
CaO %	0.30	0.26	0.20	0.41	0.25	0.33	0.21	0.43	0.33	0.54	0.23	0.75	0.43
Na_2O %	3.18	3.69	3.56	3.78	3.23	3.36	3.16	3.12	2.77	2.94	2.74	3.20	3.12
K_2O %	5.11	4.91	4.96	4.73	5.51	5.01	4.95	4.91	4.92	5.16	5.08	4.94	4.83
TiO_2 %	0.13	0.10	0.10	0.09	0.16	0.16	0.14	0.13	0.13	0.14	0.16	0.10	0.10
P_2O_5 %	<0.05	<0.05	<0.05	<0.05	<0.05	<0.05	<0.05	<0.05	<0.05	<0.05	<0.05	<0.05	<0.05
MnO %	0.06	0.06	0.05	0.07	0.04	0.05	0.07	0.06	0.06	0.03	0.08	0.07	0.08
LOI %	0.42	0.30	0.81	0.43	0.87	0.41	1.19	1.11	1.70	1.54	1.12	1.20	1.57
F %	0.04	0.02	0.07	0.28	0.02	---	0.02	0.09	0.03	0.03	0.01	---	0.15
total%	98.92	98.59	99.20	98.50	98.46	99.88	99.56	99.38	99.21	98.79	98.33	99.17	98.59
O F %	0.02	0.01	0.03	0.12	0.01	---	0.01	0.04	0.01	0.01	0	---	0.06
Total%	98.90	98.58	99.17	98.38	98.45	99.88	99.55	99.34	99.20	98.78	98.33	99.17	98.53
Sn ppm	<4	5	20	7	70	4	12	<4	25	<4	46	2	2

	1	1A	2	2A	3	3A	4	4A	5	5A	6	7	8
As ppm		<10		<10				<10		10			
B	<20	--	<20	--	<20	30	<20	--	<20	--	<20	<20	<20
Ba	15	25	30	63	30	70	20	17	15	14	15	30	15
Be	10	10	5	6	5	15	10	10	5	10	7	3	7
Cu	3	3	3	7	2	2	3	7	2	5	2	7	3
Mo	<3	5	3	3	3	7	5	4	<3	5	5	3	5
Nb	30	16	30	16	30	70	30	18	30	17	30	30	30
Ta	--	4	--	3	--	--	--	5	--	5	--	--	--
Pb	20	28	15	48	20	70	20	30	20	35	30	15	20
Sc	<5	<2	<5	3	<5	5	<5	<2	<5	<2	<5	5	<5
Sr	<5	4	5	10	7	15	<5	3	<5	5	<5	5	<5
U	--	10	--	12	--	--	--	17	--	17	--	--	--
Th	--	31	--	31	--	--	--	28	--	38	--	--	--
V	<7	<2	<7	15	<7	15	<7	<2	<7	87	<7	<7	15
Zn		40		50				60		50			
Zr	150	210	150	170	150	300	150	120	150	180	150	300	150
Cs	--	3	--	4	--	--	--	3	--	4	--	--	--
Hf	--	7	--	8	--	--	--	8	--	8	--	--	--
Rb	--	444	--	292	--	--	--	396	--	400	--	--	--
Ga	30	18	30	17	30	50	30	19	30	19	30	30	30
Li	<100	50	<100	34	<100	<100	<100	53	<100	55	<100	<100	<100
La	30	35	<30	71	50	100	<30	15	30	33	70	50	50
Ce	<200	77	<200	150	<200	300	<200	40	<200	72	<200	<200	<200
Nd	<70	29	--	62	<70	70	--	0	<70	31	<70	<70	<70
Sm	<100	7	--	15	<100	<100	--	2	<100	8	<100	<100	<100
Eu	<100	.2	--	.5	<100	<100	--	.2	<100	.2	<100	<100	<100
Gd	<50	9	--	16	--	<50	--	3	<50	10	<50	<50	--
Tb	<300	1	--	2	--	<300	--	.2	<300	1	<300	<300	--
Tm	<20	1	--	1	--	<20	--	0	<20	1	<20	<20	--
Yb	10	7	5	12	5	15	2	3	7	9	7	7	7
Lu	<30	1	--	1	--	<30	--	.5	<30	1	<30	<30	--
Y	70	64	50	110	50	100	10	13	70	70	70	70	50

	9	10	11	12	13	14	15	16	17	18	19	20	21
As ppm	<10						<10	<10	20	<10	120		
B	--	50	50	70	20	15	--	--	--	--	--	15	30
Ba	97	30	15	7	70	70	58	67	57	76	44	20	30
Be	7	15	15	15	7	7	7	7	7	7	6	10	15
Cu	3	2	5	3	5	2	7	6	4	6	7	3	1
Mo	2	15	7	15	15	<3	3	2	3	3	2	3	<3
Nb	21	50	70	150	50	30	24	23	25	17	10	30	70
Ta	4	--	--	--	--	--	4	3	4	3	3	--	--
Pb	29	30	70	70	150	15	30	21	23	32	50	30	30
Sc	3	5	<5	<5	7	<5	2	3	2	2	<2	<5	<5
Sr	11	10	10	7	70	30	9	21	15	39	52	30	30
U	11	--	--	--	--	--	22	8	17	16	11	--	--
Th	33	--	--	--	--	--	31	29	31	29	34	--	--
V	4	30	15	<7	30	15	4	2	5	4	6	<7	<7
Zn	100						40	70	50	30	40		
Zr	150	150	300	300	200	300	130	140	140	170	140	200	200
Cs	5	--	--	--	--	--	7	7	5	5	14	--	--
Hf	8	--	--	--	--	--	7	7	7	7	7	--	--
Rb	330	--	--	--	--	--	340	314	310	320	346	--	--
Ga	19	70	50	70	30	30	17	18	16	18	17	30	70
Li	39	<100	<100	150	<100	<100	40	38	37	23	22	100	150
La	45	150	70	150	150	70	41	48	49	39	66	70	100
Ce	107	300	150	300	200	150	110	110	110	95	130	150	200
Nd	44	100	70	150	100	70	39	46	44	32	49	70	100
Sm	11	<100	<100	<100	<100	<100	9	12	12	7	12	<100	<100
Eu	.3	<100	<100	<100	<100	<100	.3	.4	.3	.3	.4	<100	<100
Gd	14	<50	<50	<50	<50	<50	9	14	13	7	16	<50	<50
Tb	2	<300	<300	<300	<300	<300	1	2	2	1	3	<300	<300
Tm	1	<20	<20	<20	<20	<20	1	1	1	1	2	<20	<20
Yb	8	15	15	20	15	7	8	10	11	6	15	20	20
Lu	1	<30	<30	<30	<30	<30	1	1	2	1	2	<30	<30
Y	62	150	100	200	150	70	54	110	93	48	74	150	150

1. NE,NE,Sec.33 T8S R11W, flow near Indian Peak
1A. NE,NW,Sec. 6 T9S R11W, flow on Indian Peak
2. NW,NE,Sec.34 T9S R11W, flow N. of Squaw Cr.
2A. NW,NW,Sec.35 T9S R11W, flow N. of Squaw Cr.
3. NW,NW,Sec.33 T9S R10W, flow in Hardcastle Cr.
3A. SW,SW,Sec.28 T9S R10W, flow S. of Nugget Gl.
4. SW,SW,Sec.12 T10S R11W, flow near Squaw Peak
4A. do
5. SW,NE,Sec.18 T10S R10W, flow near Boiler Peak
5A. NW,SE,Sec.18 T10S R10W, flow on Boiler Peak
6. NW,NW,Sec.25 T10S R11W, flow in Taylor Creek
7. SE,SW,Sec. 4 T11S R10W, flow near 74 Draw
8. SW,NE,Sec. 1 T11S R11W, flow near Alexander Pk.
9. NE,SW,Sec. 5 T11S R12W, flow on Kemp Mesa
10. SW,NE,Sec.17 T10S R10W, froth flow, Sawmill Cr.
11. SW,NE,Sec.19 T10S R10W, altered flow, Sawmill Cr.
12. SE,SE,Sec.19 T10S R10W, vitrophyre, N. Scales Cr.
13. SE,SW,Sec. 4 T11S R10W, flow near 74 Draw
14. NW,NW,Sec.31 T11S R6W, flow, Willow Spring Draw
15. NE,SW,Sec. 5 T11S R12W, vapor-phase crystallization
16. SW,SW,Sec. 5 T11S R12W, do, Kemp Mesa area
17. do
18. SE,SW,Sec.34 T9S R11W, do, Squaw Creek adit
19. do
20. SE,SE,Sec.23 T10S,R11W, vapor-phase alteration
21. NE,SW,Sec.30 T10S R10W, do, Scales Cr.

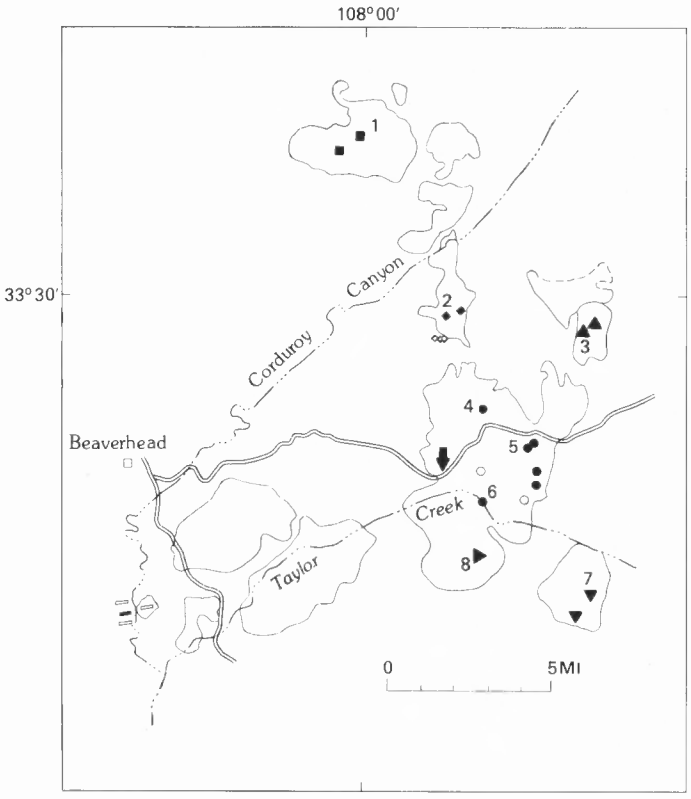


FIGURE 2—Index map of sample localities. Symbols are keyed to graphic representation of analytical results shown in Figs. 3 and 4. Numbers refer to locations for samples dated by K–Ar method (Tab. 2). Solid symbols represent unaltered rock with minimum devitrification and one vitrophyre; open symbols represent rocks with vapor-phase crystallization or complete devitrification.

temperature, low-pressure, vapor-dominated systems to lower-temperature, lower-pressure, fluid-dominated systems. The deposit at Stop 5 of First Day is typical of a high-temperature, low-pressure, vapor-dominated system. Other deposits, initially vapor-dominated, grade into lower-temperature fluid-dominated systems, as at Squaw Creek (Fig. 1, no. 2). The larger deposits, such as those at Sawmill Creek (no. 4), Nugget Gulch (no. 3), and Juniper (no. 1) are fluid-dominated, variable in temperature, chemically complex, and show multiple cycles of mineralization. Still other deposits appear to have formed at ambient temperature and pressure, and are possibly supergene. Tin occurrences are informally divided into four corresponding types to facilitate discussion.

Type I consists of small crystals of cassiterite in lithophysae, miarolitic cavities, and tiny gash veins in association with specular hema-

TABLE 2—K–Ar age determinations on sanidine from eight samples of Taylor Creek Rhyolite. Age determinations made by R.F. Marvin, H.H. Mehnert, and E.L. Brandt of the USGS (written comm. 1985). Numbered localities are shown in Fig. 2.

Location	Age in my
1. Indian Peaks	26.3 ± 1.7
2. Squaw Creek	25.9 ± 0.9
3. Hardcastle Creek	25.7 ± 0.9
4. Squaw Peak	25.9 ± 2.1
5. Boiler Peak	25.0 ± 0.9
6. Taylor Creek	25.9 ± 0.9
7. 74 Draw	26.6 ± 1.0
8. Alexander Peak	27.3 ± 1.0

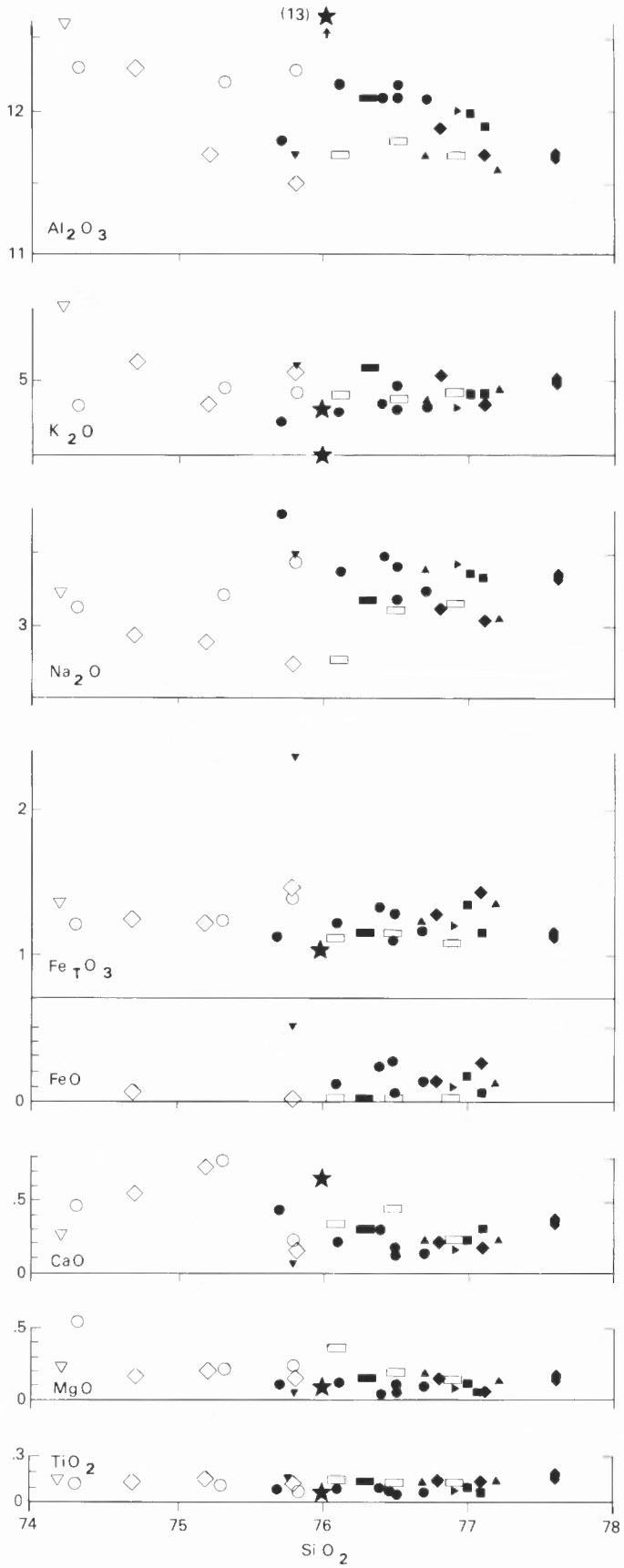


FIGURE 3—Harker diagram of analyses of Taylor Creek Rhyolite. Symbols correspond to those in Fig. 2. Star is average topaz rhyolite (Christiansen et al. 1983: 18), symbol on far right is from the Willow Creek deposit, Monticello tin area.

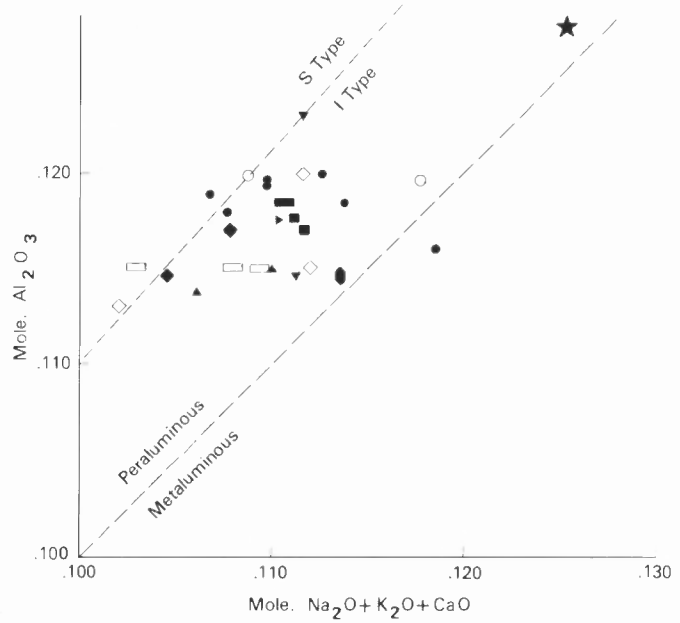


FIGURE 4—Alumina–alkali plot of analyses of Taylor Creek Rhyolite samples. S-I type line derived from Chappell & White (1974). Symbols are same as in Fig. 3.

tite, pseudobrookite, bixbyite, topaz, quartz, and sanidine. The gash veins generally have thin seams of tabular hematite with sparse, thin coatings of cassiterite and, rarely, crystalline cassiterite interstitial to hematite.

Type II consists of well-defined gash veins and anastomosing veinlets that vary widely in orientation and size. Individual veinlets are generally less than 1 cm thick and 1 m long, but locally may be as much as 10 cm thick and 8 m long. Veinlets are composed mostly of thin plates of specularite coated by and/or replaced by cassiterite. Associated minerals include quartz, fluorite, sanidine, zeolites, and several rare or unnamed fluoroarsenates, arsenates, and antimonates. Wall rock is sometimes altered and mineralized for several centimeters adjacent to the veinlets. Hematite and cassiterite are locally finely disseminated in the wall rock in bands reminiscent of liesegang banding.

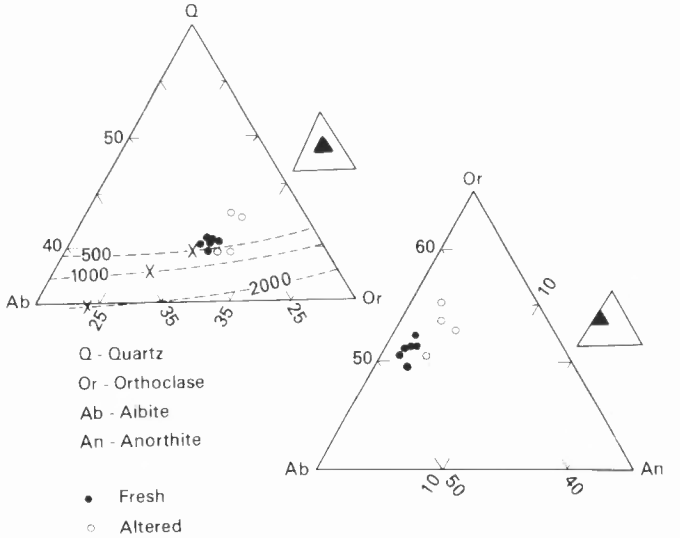


FIGURE 5—Ab–Or–Q and Ab–An–Or ternary diagrams for samples of Taylor Creek Rhyolite calcualted from rock norms. Ternary thermal minima (x) are indicated for 500, 1,000, and 2,000 isobaric (quartz–feldspar boundary) lines. After Tuttle & Bowen (1958: 75). Solid dots represent rocks showing minimum devitrification; open circles represent rocks showing variable vapor-phase crystallization.

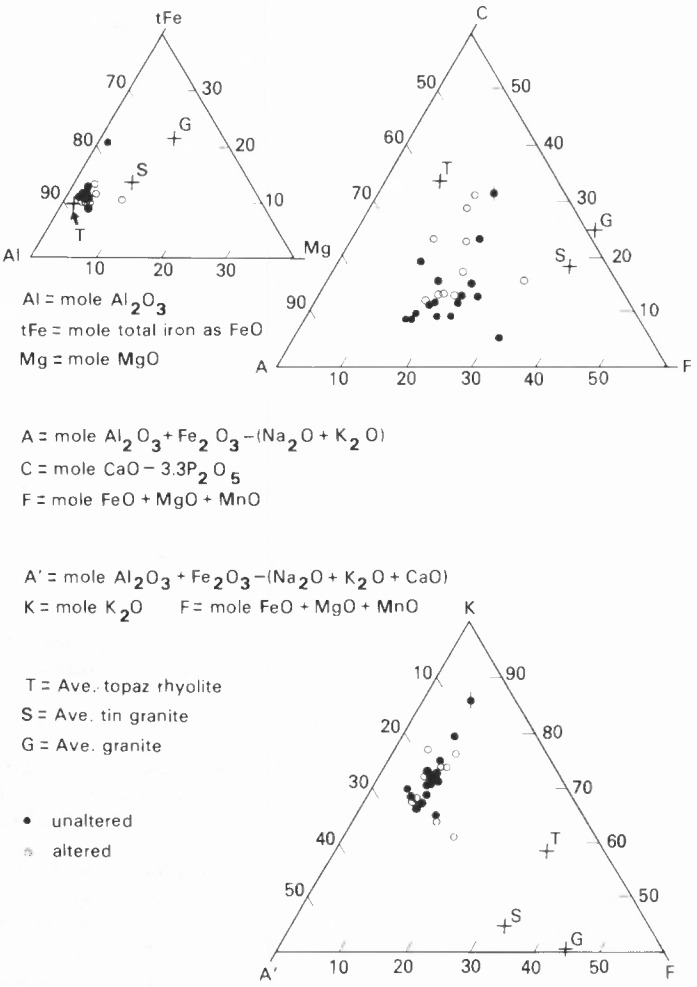


FIGURE 6—AFM, ACF, and A'KF plots of major-oxide analyses of Taylor Creek Rhyolite. Average topaz rhyolite from Christiansen et al. (1983), average tin granite and average granite from Stemprok & Skvor *in* Taylor (1979: 90–91). Solid dots represent rocks with minimum devitrification; dot with vertical line is a vitrophyre; open circles represent rocks showing vapor-phase crystallization.

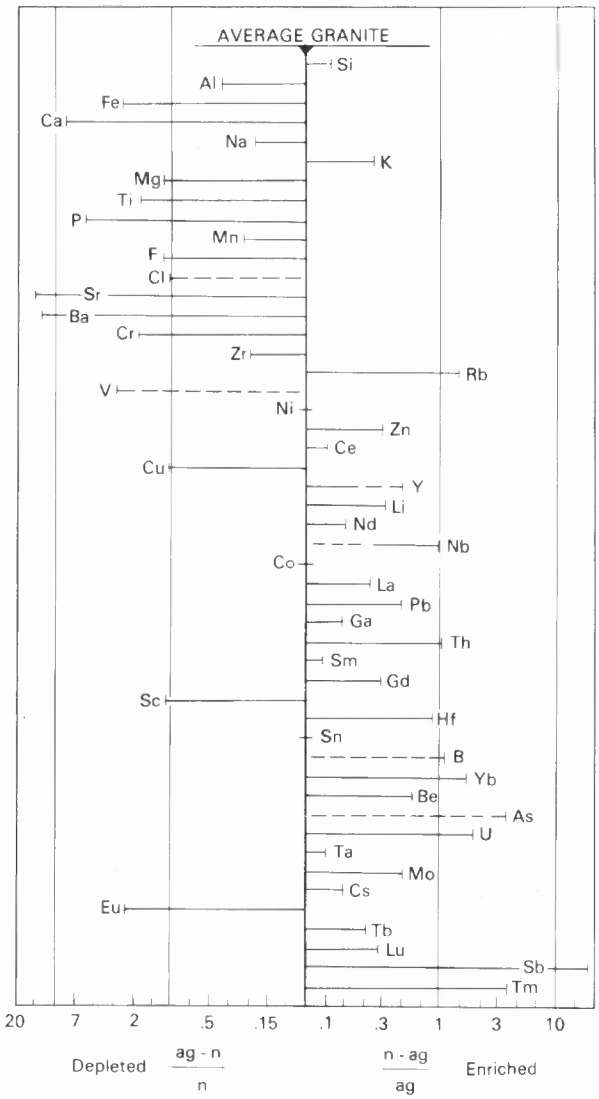


FIGURE 7—Diagram showing relative ratios of depletion or enrichment of elements in Taylor Creek Rhyolite compared to concentration in an average granite (Krauskopf 1979). ag = average granite, n = average amount in Taylor Creek Rhyolite.

Type III is the most complex and occurs in veins and stockwork-like areas of reticulate veinlets in the distal edges of the rhyolite flow domes and in the underlying tuffs and ash-flow tuffs. Some veins may be as much as 30 or 40 cm wide and extend 100 m or more; the zones of reticulate veinlets may be several thousand square meters in size, with veinlets spaced a few tens of centimeters to several meters apart, and with much of the intervening rock altered and mineralized. The associated minerals include hematite, cassiterite, wood-tin, durangite, beudandite, hidalgoite, jarosite, alunite, cristobalite, tridymite, quartz, chalcedony, hyaline opal, fluorite, smectite, cryptomelane, and todorokite.

There is a possibility of a fourth type, which may be supergene accumulations of wood-tin and varlamoffite(?). The wood-tin occurs in porous zones in sandstone, conglomerate, and tuff associated with limonite staining and in subsurface pockets of intensely altered or weathered rock, most commonly in pockets filled with red clay. Deposition of wood-tin and/or macrocrystalline cassiterite under surface conditions has been documented previously (e.g. Hanks 1876: 276, Palache et al. 1944: 577, 579).

The tin-bearing veins, particularly those occurring in type III deposits, contain distinctly elevated amounts of F compared to the host volcanic rocks. Fluorine in type I deposits is principally contained in topaz, while types II and III are characterized by the presence of some or all of the following fluorine-bearing minerals: fluorite, durangite, topaz, and several as yet incompletely described fluoroarsenates.

Cassiterite, which has a nominal formula of SnO_2, occurs in several different forms throughout the district, with certain of the forms predominant in individual deposits. Crystals of cassiterite can be nearly black, dark brown or red, bright red, orange, yellow, light tan, amber, and rarely almost colorless. The most common form is dark red, pseudomorphic after hematite, in bladed aggregates intergrown with hematite, often almost completely replacing the hematite. Less common are euhedral crystals or aggregates of crystals. Individual crystals are generally small, 0.5–3 mm in maximum dimension and rarely as much as 5 mm across. Crystals disseminated in the highly altered wallrock in some localized areas are only a few microns in diameter.

Some of the dark-red cassiterite has numerous inclusions of hematite, but most crystals have no discernible inclusions at 0.1 micron. Analyses of carefully cleaned crystals from several different localities and from different positions in the paragenetic sequence gave results that varied from essentially pure SnO_2 to material with as much as 10 wt% of Fe, Sb, As, Zn, In, Si, and other elements. Similar results were obtained from more than 100 microprobe analyses of wood-tin and crystalline tin from several localities. Samples of wood-tin from Juniper (Fig. 1,

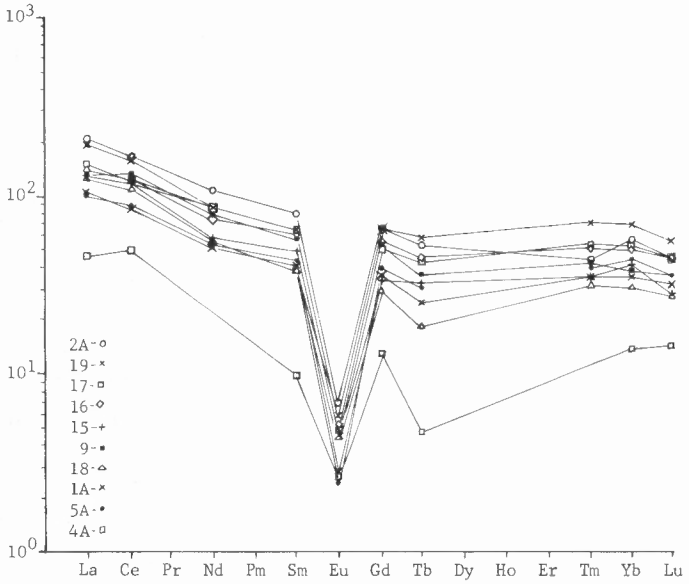


FIGURE 8—Chondrite-normalized REE plot for selected samples of Taylor Creek Rhyolite. Sample numbers are the same as in Tab. 1. (Bruce Reed written comm.)

no. 1), Nugget Gulch (no. 3), and Sawmill Creek (no. 4) contain approximately 0.2 wt% H_2O. Cassiterites from each of the four deposit types have distinctive chemical characteristics. A relatively consistent variation in content of isomorphously substituting elements, such as those listed above, occurs over the paragenetic sequence and from one locality to another. Erratic variations in some of the elemental concentrations might be explained wholly or in part by crystal zoning. At one locality, and perhaps others, very sparse amounts occur of what appear to be either zoned crystals of an Sb-, Sn-, Fe-, and Ti-bearing monoclinic modification of the tirutile structure having the formula $(Sb,Sn,Fe,Ti)_3O_6$, or tripuhyite ($FeSb_2O_6$). This material may or may not grade in composition over a distance of only a few microns to iron- and antimony-bearing cassiterite.

Carefully cleaned separates of many of the different minerals listed above were analyzed for their element content, and some were polished and studied with the electron microprobe. A specimen of thick tabular hematite had small exsolution blebs of cassiterite aggregating less than 1% Sn; none of the other minerals studied showed exsolution-type textures. All of the minerals, but especially the cassiterite, showed variable and generally moderate to large amounts of elemental substitution.

Almost all of the tin produced in the district was from placer or colluvial deposits, as wood-tin nuggets derived from underlying or nearby veins. Some of the nuggets are bladed aggregates of crystalline cassiterite and hematite, others are vaguely laminated, fine-grained mosaics of cassiterite and hematite, which originally may have been wood-tin and then recrystallized to its present form (Pan 1974). Many of the nuggets are cryptocrystalline wood-tin characterized by parallel thin laminae of contrasting colors that closely resemble the growth rings of wood.

TABLE 3—Comparison of selected elemental concentrations in tin-granite and Taylor Creek Rhyolite. Values are in ppm. Values for Sn-granite from Tischendorf *in* Taylor (1979: 114). Value for Li shown in parentheses from Tourtelot & Meier (1976).

	Tin-granite	Average Taylor Creek Rhyolite
F	3700 ±1500	575
Rb	580 ±200	345
Li	400 ±200	39.1 (38)
Sn	40 ±20	4.6
Be	13 ±5	8
W	7 ±3	3
Mo	3.5 ±2	3

Wood-tin occurs in veins and adjacent altered host rock as rounded single masses a few millimeters to 6 cm in diameter, as botryoidal aggregates and stalactite-like botryoids of similar size, commonly with a core of host rock, and as botryoidal or undulating slabs as much as 16 cm across and 3 cm or more thick. Wood-tin may also occur as irregularly rounded masses of botryoids intergrown with hematite and amorphous silica. The largest such mass found by the authors is 10×15 cm and weighs 4.5 kilos (10 pounds).

Toad's-eye tin is locally very common in the larger veins, late in the paragenetic sequence. It is commonly hemispherical or spherical, composed of small acicular reddish or yellowish-brown cassiterite crystals radiating from a center. They are generally 3 or 4 mm in diameter, but range from 1 to 10 mm. A similar but loose aggregation of acicular cassiterite "fuzz-balls" is locally common as the last mineral deposited in vein cavities. These aggregates are white or light tan and are at most a few millimeters in diameter. The balls are compact masses in the center which radiate outward to individual flexible fibers commonly less than 1 micron in diameter. Some of the masses are just a loose aggregate of fibers.

Certain laminae on the outer surfaces of some wood-tin nuggets, from a few specific localities, are light green or greenish tan, soft, and waxy. They are nearly x-ray amorphous and might be varlamoffite $(Sn,Fe)(O,OH)_2$. Such material often recrystallizes to cassiterite over a period of a few years when removed from a hydrous environment.

Single cassiterite crystals and cassiterite crystals on wood-tin nodules from one locality about 3 km northwest of Locality 4 (Fig. 1) were studied for fluid-inclusion homogenization temperatures. Such temperatures ranged from 347 to 417°C, with 60% of the temperatures ranging from 365 to 380°C (Harvey 1985).

Oxygen isotopes of selected mineral specimens from the Black Range tin deposits indicate crystallization temperatures of more than 500°C for minerals in the miarolitic cavities, decreasing in later minerals. Cassiterite in miarolitic cavities may be related to outgassing of the domes, but most tin mineralization probably occurred after the domes had cooled, deposited in a near-surface environment from magmatic deuteric fluids derived from an underlying magma source (Rye et al. 1984).

Eggleston & Norman (1984) state that some cassiterite was deposited at 150–200°C from boiling fluids with a calculated δO^{18} of -6 to 0 permil, and suggest that both magmatic and meteoric fluids were involved in tin deposition and that wood-tin was deposited from meteoric-water-dominated, epithermal systems.

Descriptions of selected deposits and occurrences

The deposits (types I and II) at Squaw Creek (Fig. 1, no. 2) are exposed by trenches and a short adit. Several small gash veins and an intermittent vein several meters long are exposed. The vein minerals are predominantly platy hematite and red euhedral cassiterite, locally coated with various forms of silica, sanidine, or heulandite. Miarolitic cavities adjacent to the veins contain euhedral red and amber cassiterite. Cavities 1–2 cm from the vein outward for 20–50 cm are lined with tridymite, sparse pseudobrookite, and several rare and new minerals. The new minerals include antimonates, arsenates, and fluoroarsenates. Unfortunately, the new minerals are very sparse and tiny, making mineralogical studies exacting and difficult. Work is currently in progress by Gene Foord, Paul Hlava, and others to describe and name the minerals. Several blocks of altered rhyolite between veins and fractures have irregular annular bands of red interstitial cassiterite, mixed cassiterite and hematite, and hematite in a configuration similar to liesegang banding.

A lower adit was driven to intersect the veins below the Squaw Creek trenches, but none were exposed. Here the rhyolite showed much stronger vapor-phase alteration, with tridymite and sanidine in cavities. Several

fractures were stained with limonite and filled with a reddish-brown smectite that contains anomalous amounts of tin and rare-earth elements along with arsenic and antimony.

The deposits (type II) at Alexander (Fig. 1, no. 5) are in a carapace breccia exposed in three short adits and several small trenches. The veinlets are mostly fine-grained, platy hematite locally coated with brown clay. Deposition in the larger veins starts with early large, blocky, euhedral hematite followed by thin, platy hematite and thin arborescent hematite cores in black euhedral crystals of cassiterite. The cassiterite is amber in thin splinters and contains about 9 wt% Sb_2O_5, 6 wt% Fe_2O_3, and approximately 0.3 wt% MnO (Fig. 9). The hematite and cassiterite are covered with botryoidal and stalactitic cristobalite. Pink, coarsely crystalline, dioctahedral smectite formed interstitially to the stalactitic cristobalite. The smectite contains 0.8% REE, 0.3% Zn, and anomalous amounts of Sn. Thin, platy hematite and euhedral cassiterite locally grew on the smectite. Other parts of the larger veins have a coarsely crystalline, granophyric mixture of sanidine and quartz coated with blocky to thin, platy hematite and large (up to 5 mm) transparent crystals of sanidine with the morphology of adularia. The sanidine crystals are optically and microprobe homogeneous, with albite molecule about equal to orthoclase.

The deposits (types II and III) at 74 Draw (Fig. 1, no. 6) are in the distal edge of a rhyolite flow and are well exposed in a shaft and several trenches. Most of the veins are hematite or hematite and clinopyroxene, locally with sparse fine-grained cassiterite coating the hematite. A few veins or segments of veins are more complex, with a paragenetic sequence of hematite, cassiterite, fine-grained hematite, cassiterite, durangite, cristobalite, fluorite, and smectite, with hydrothermal alteration of the wallrock 10–20 cm on either side of the veins. The clinopyroxene crystals are orange, brownish red, and alexandrite-like in color.

The deposits (type II) at Taylor Creek and Kemp Mesa–Beaver Creek (Fig. 1, nos. 7, 8) are similar, with hematite and hematite–cassiterite veins, some with small amounts of wood-tin. The area also contains several zones of highly altered rock with widely disseminated, tiny cassiterite crystals. These zones were developed by several long adits and numerous shafts.

The veins at the Juniper locality (Fig. 1, no. 1) (type III) are exposed in trenches, washes, and in shallow scraped areas (Fig. 10). One vein can be traced for more than 100 m by a line of cassiterite and hematite fragments in the soil. Removal of a few centimeters of soil reveals the vein. Veins in the area range from a few to 30 cm or more in thickness and tin content varies from miniscule to major. Thicker segments of tin veins show at least six cycles of deposition, each a centimeter or more in thickness: hematite, cassiterite, hematite, cassiterite, hematite, and a complex grouping of cassiterite, beudantite, jarosite, cristobalite, fluorite, and smectite. The early cassiterite contains 3% Sb and less than 0.01% Zn; the latest cassiterite contains 0.1% Sb and 0.07–0.1% Zn (Fig. 9), a pattern repeated at other localities.



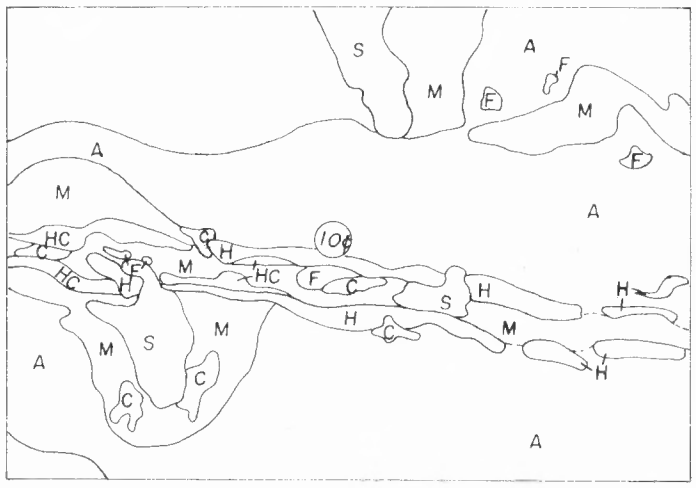


FIGURE 10—Tin vein exposed in a wash at Juniper (Fig. 1, no. 1). H = hematite; C = cassiterite, mostly wood-tin; HC = intergrown hematite and cassiterite crystals; F = fluorite with varying amounts of cristobalite and smectite; S = dark-red smectite; M = fine-grained mixtures of all the above; A = altered host rock, mostly smectite.

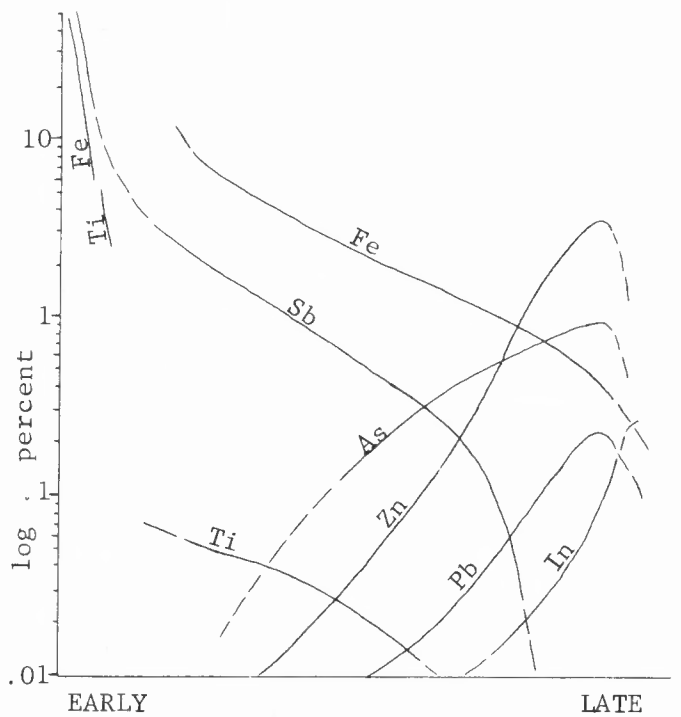


FIGURE 9—Diagram showing generalized trend lines of extraneous element variation in cassiterite relative to paragenetic sequence.

Many interesting areas of silicification occur around the Juniper deposits, mostly to the east and south (Richter & Lawrence 1986). They appear to be hot-spring sinter deposits composed mostly of chalcedony and opal, with fluorite coating some cavities. The sinter contained anomalous amounts of several elements: F 16%, Mn 0.3%, Bi 700 ppm, Mo 70 ppm, Pb 0.7%, Zn 0.15%, V 700 ppm, Sn 0.1%, and REE 50–500 ppm of each. A drill hole on one of the sinter deposits (small dot SW of no. 1, Fig. 1) had similar anomalies in the top 7–10 m: F 2–7%, Bi 300 ppm, Pb 1.5%, Sn 0.1–0.2%; lead and zinc were anomalous to 130 m.

The Nugget Gulch area (Fig. 1, no. 3) (types III and IV) was extensively explored in 1939–1940 (Fries 1940, Volin et al. 1947) by numerous shafts, adits, and trenches. In the 1960's and 70's most of the placer tin was removed from an area of about 5,000 m^2. This scraping

revealed bedrock and numerous veinlets within a portion of a west–northwest-trending zone about 1 km long and 200 m wide.

Most veinlets exposed in the Nugget Gulch area are small, less than 1 cm wide. Some are predominantly hematite in thin plates, some have hematite, cassiterite crystals, and wood-tin, but most have only wood-tin. Most of the wood-tin nodules are dark brown in the center, grading outward to tan at the surface; a few have a thin black layer at the surface. The earliest cassiterite contains about 9% Fe, 0.7% Sb, 0.1% Mn, and minor Zn and As. The wood-tin has as much as 10% FeO in the cores, grading outward to less than 1% in the rims, 1–1.5% As_2O_3 and 2–4% Sb_2O_5 in the central part, and as much as 3% ZnO and 3% SiO_2 in the outer rims (Fig. 9). In_2O_3 is locally present in amounts exceeding 2% (Lufkin 1977). Very large pieces of vein material in the alluvium, as much as $16 \times 12 \times 7$ cm, indicate the presence of veins much larger than those currently exposed.

Deposits (types III and IV) near the headwaters of Sawmill Creek (Fig. 1, no. 4) are exposed by numerous shallow trenches. One area of about 6,000 m^2 was scraped off and washed clean with a high-pressure water jet in the late 1960's, revealing a reticulate network of many veinlets and a few small veins of variable thickness, each with an envelope of hydrothermal alteration. After a few years the surface had weathered to thin soil, obscuring most of the veinlets and allowing the growth of many small pine trees.

A generalized paragenetic sequence of the veins is shown in Fig. 11. This paragenetic sequence is highly variable, subject to just about every permutation conceivable. Adjacent altered wall rocks contain fluorite, barite, cristobalite, durangite, smectite, todorokite, and locally disseminated cassiterite. The durangite ($NaAlAsO_4F$) here is the fourth recorded world occurrence (Foord et al. 1985).

A specimen of wood-tin from the Sawmill Creek clearing was nearly pure SnO_2, with only trace amounts of Fe, W, and Mn. Crystalline cassiterite contained 5–7% Fe, 0.7% Sb, and minor W, Mn, and Zn (Fig. 9).

Discussion

Many areas of intense vapor-phase alteration in the flow domes have no associated deposits or occurrences of cassiterite, even though rocks favorable for deposition are present. The paucity of cassiterite in a few vapor-dominated deposits that are present shows that only a small amount of tin was deposited at those localities during degassing of the rhyolite. Analyses of rocks that are nearly all vitrophyre, with only a little devitrification showing, contained 1–5 ppm tin, and one vitrophyre contained 7 ppm, an order of magnitude less than a normal tin rhyolite and little more than average crustal abundance for granitic rocks (Fig. 7).

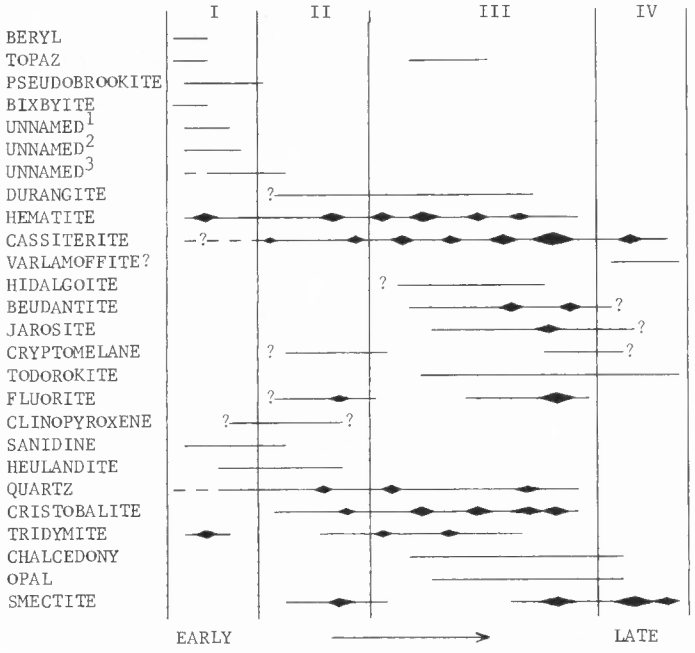


FIGURE 11—Generalized paragenetic sequence of cassiterite and associated minerals in Black Range tin district. The unnamed minerals are currently being named and described. Unnamed[1] is an Sb–Sn–Fe–Ti oxide related to cassiterite, unnamed[2] is a yellow Ce-group arsenate, and unnamed[3] is a red Na–Ca–Fe–Mn–Mg fluoroarsenate.

More than 90% of the tin in the district occurs in fluid-dominated vein systems which show multiple cycles of deposition and are located on the distal edges of the Taylor Creek Rhyolite and underlying pyroclastics. A fair proportion of this tin is in older rocks several kilometers away from the closest dome. Cassiterite is associated with a carapace breccia at only one locality (Alexander, Fig. 1, no. 5) of all those studied.

Vapor-domianted occurrences (type I) and perhaps some of the type II occurrences as well appear to be derived from the domes. The remaining part of type II were fluid-dominated, most likely derived in part from the flow domes themselves and in part from the underlying intrusive in the conduit. Type III deposits appear to be representative of a deeper source, perhaps in part from the same rhyolite in the conduit, but mostly from the parent magma, and deposited from magmatically derived deuteric fluids at a vertically telescoped interface, at a steeper temperature gradient. These deuteric fluids most likely interacted to varying extent with meteoric ground water. Cassiterite from type IV deposits has been formed under ambient conditions. Distinctive elemental associations with some elements present throughout the crystallization history of the four types of tin deposits are evident (Figs. 9, 11). Iron and tin are present in all four types of deposits. Sb, Ti, and Mn are diagnostic elements in type I deposits. Type II deposits are distinguished by the presence of Sb and As. The chemically most complex deposit type (III) contains As, Pb, Zn, W, Mo, Bi, and V along with abundant F. This association of elements is interpreted to have come from epigenetic sources. Type IV deposits contain only Sn, Fe, and Mn.

Conclusions

The tin deposits were derived from a granitic rock with only a normal or very slightly enriched tin content, and were concentrated and deposited by a combination of favorable geologic conditions.

The Taylor Creek Rhyolite had been in place and cooled before the influx of magmatic hydrothermal fluids that produced the largest deposits. Some allied hydrothermal (hot-spring) fluids formed tin-bearing siliceous sinter deposits near current topographic levels, possibly during Holocene time.

ECONOMIC SUMMARY

Most of the occurrences of tin (Fig. 1) are of types I, II, and IV and are too small to have much resource potential. Three areas of type III occurrences (Fig. 1, open circles) contain mineable deposits. Individual veins of type III are relatively rich in tin, but are impractical to mine separately. The areas containing closely spaced veins and veinlets are large but low-grade; analyses of channel samples and grid samples of two areas and chip traverses across others gave an average tin content of about 0.1%, and would be amenable to bulk mining. Several such areas have 20,000–60,000 m^3 of mineralized rock with an inferred aggregate total of about 5 million tons with nearly 0.1% recoverable tin. Estimates are based on a few drill holes that indicate a thickness of 6–10 m of mineralized rock, below which the tin content decreases to 20–200 ppm.

ACKNOWLEDGMENTS

We gratefully acknowledge the many colleagues who aided in this study. Special appreciation goes to Robert C. Kerr of Truth or Consequences for his hospitality and inestimable assistance in the studies. We also wish to express our appreciation to the ranchers in the region, especially the very helpful and hospitable people at Adobe Ranch. Much of the chemical analytical work was done by our colleagues in the Branch of Analytical Chemistry, USGS. We wish to acknowledge the contributions of N.M. Conklin, J.E. Seeley, and Leon Bradley (emission spectrographic analyses), J.E. Taggart, K.A. Stewart, and A.J.

Bartel (XRF majors), and L. Jackson and S. Wilson (waters and F). We also wish to thank E.A. duBray, H.R. Stein, and P.J. Modreski for their prompt and perceptive reviews.

REFERENCES

Burt D.M., Sheridan M.F., Bikun J.V. & Christiansen E.H. 1982. Topaz rhyolites—distribution, origin, and significance for exploration.—Economic Geology, 77: 1818–1836.

Chappell B.W. & White A.J.R. 1974. Two contrasting granite types.—Pacific Geology, 8: 173–174.

Christiansen E.H., Burt D.M., Sheridan M.F. & Wilson R.T. 1983. The petrogenesis of topaz rhyolites from the western United States.—Contributions to Mineralogy and Petrology, 83: 16–30.

Correa B.P. 1980. Fluorine and lithophile element mineralization in the Black Range and Sierra Cuchillo, New Mexico. *In* Burt D.M. & Sheridan M.F. (eds.), Uranium mineralization in fluorine-enriched volcanic rocks.—U.S. Department of Energy, Report GJBX-225-80: 459–494.

Correa B.P. 1981. The Taylor Creek Rhyolite and associated tin deposits, southwestern New Mexico (M.S. thesis).—Arizona State University, Tempe, 105 pp.

Eggleston T.L. (in preparation). Geology and geochemistry of Taylor Creek tin district, Black Range, New Mexico (Ph.D. thesis).—New Mexico Institute of Mining & Technology, Socorro.

Eggleston T.L. & Norman D.I. 1983. Taylor Creek tin district—stratigraphy, structure, and timing of mineralization.—New Mexico Geology, 5(1): 1–4.

Eggleston T.L. & Norman D.J. 1984. Geochemistry and origin of rhyolite-hosted tin deposits, southwestern New Mexico (abstract).—Geological Society of America, Abstracts with Programs, 16(6): 499.

Elston W.E. 1968. Terminology and distribution of ash-flows of the Mogollon–Silver City–Lordsburg region, New Mexico.—Arizona Geological Society, Guidebook III to southern Arizona, pp. 231–240.

File L. & Northrop S.A. 1966. County, township, and range locations of New Mexico's mining districts.—New Mexico Bureau of Mines & Mineral Resources, Circular 84: 66 pp.

Foord E.E., Oakman M.R. & Maxwell C.H. 1985. Durangite from the Black Range, New Mexico, and new data on durangite from Durango and Cornwall.—Canadian Mineralogist, 23: 241–246.

Fries C. Jr. 1940. Tin deposits of the Black Range, Catron and Sierra Counties, New Mexico.—U.S. Geological Survey, Bulletin 922-M: 355–370.

Fries C. Jr. & Butler A.P. 1943. Geologic map of the Black Range tin district, New Mexico.—U.S. Geological Survey, open-file map.

Fries C. Jr., Schaller W.T. & Glass J.J. 1942. Bixbyite and pseudobrookite from the tin-bearing rhyolite of the Black Range, New Mexico.—American Mineralogist, 27: 305–322.

Goerold W.T. 1981. Geology and geochemistry of tin occurrences in southwestern New Mexico (M.S. thesis).—Pennsylvania State University, University Park, 131 pp.

Hanks H.G. 1876. On the occurrence of durangite in the tin-bearing region of Durango, Mexico.—American Journal of Science (3), 12(70): 274–276.

Harley G.T. 1934. The geology and ore deposits of Sierra County, New Mexico.—New Mexico Bureau of Mines & Mineral Resources, Bulletin 10: 232 pp.

Harvey D.B. 1985. Cassiterite mineralization in the Black Range tin district, Sierra and Catron Counties, New Mexico (M.S. thesis).—University of Texas at El Paso, 147 pp.

Hill J.M. 1921. The Taylor Creek tin deposits, New Mexico.—U.S. Geological Survey, Bulletin 725: 347–359.

Kimbler F.S. & Haynes P.E. 1980. An occurrence of red beryl in the Black Range, New Mexico.—New Mexico Geology, 2: 15–16.

Krauskopf K.B. 1979. Introduction to geochemistry, 2nd edition.—McGraw-Hill, New York, 617 pp.

Lawrence V.A. 1985. A study of the Indian Peaks tin-bearing rhyolite flow–dome complex, northern Black Range, New Mexico (M.S. thesis).—University of Colorado, Boulder, 112 pp.

Lawrence V.A. & Richter D.L. 1986. Geologic map of the Indian Peaks West quadrangle, Catron County, New Mexico.—U.S. Geological Survey, Miscellaneous Field Studies Map 1849, scale 1:24,000.

Lufkin J.L. 1972. Tin mineralization within rhyolite flow domes, Black Range, New Mexico (Ph.D. thesis).—Stanford University, 148 pp.

Lufkin J.L. 1976. Oxide minerals in miarolitic rhyolite, Black Range, New Mexico.—American Mineralogist, 61: 425–430.

Lufkin J.L. 1977. Chemistry and mineralogy of wood-tin, Black Range, New Mexico.—American Mineralogist, 62: 100–106.

Palache C., Berman H. & Frondel C. 1944. Dana's system of mineralogy, vol. 1.—John Wiley & Sons, New York.

Pan Y.S. 1974. The genesis of the Mexican type tin deposits in acidic volcanics (Ph.D. thesis).—Columbia University, New York, 286 pp.

Ratté J.C., Marvin R.F. & Naeser C.W. 1984. Calderas and ash flow tuffs of the Mogollon Mountains, southwestern New Mexico.—Journal of Geophysical Research, 89(B10): 8713–8732.

Richter D.L. & Lawrence V.A. 1986. Geologic map of the Indian Peaks East quadrangle, Catron County, New Mexico.—U.S. Geological Survey, Miscellaneous Field Studies Map 1850, scale 1:24,000.

Rye R.O., Lufkin J.L. & Wasserman M.D. 1984. Genesis of tin occurrences in the Black Range, New Mexico, as indicated by oxygen isotope studies (abstract).—Geological Society of America, Abstracts with Programs, 16(6): 642.

Smith R.C. 1960. Ash flows.—Geological Society of America, Bulletin, 71(6): 795–842.

Taylor R.G. 1979. Geology of tin deposits.—Developments in Economic Geology 11, Elsevier Scientific Publishing Co., New York, 543 pp.

Tourtelot E.G. & Meier A.L. 1976. Preliminary report on samples collected during lithium reconnaissance studies in the Rocky Mountains and adjacent states.—U.S. Geological Survey, Open-File Report 76-856.

Tuttle O.F. & Bowen N.L. 1958. Origin of granite in the light of experimental studies in the system $NaAlSi_3O_8$–$KAlSi_3O_8$–H_2O.—Geological Society of America, Memoir 74: 163 pp.

Volin M.E., Russell P.L., Price F.L.C. & Mullen D.H. 1947. Catron and Sierra Counties tin deposits, New Mexico.—U.S. Bureau of Mines, Report of Investigations RI-4068: 60 pp.

Woodard T.W. 1977. Geology of the Lookout Mountain area, northern Black Range, Sierra County, New Mexico (M.S. thesis).—University of New Mexico, Albuquerque, 95 pp.



Graphic mine south of Cooke's Peak, Luna County, ca 1890. Photo Henry Schmidt, New Mexico Bureau of Mines & Mineral Resources Collection, donated by R.H. Jahns.